USING STRONG SOLAR CORONAL EMISSION LINES AS CORONAL FLUX PROXIES

DAVID A. FALCONER[1], STUART D. JORDAN[2], JEFFREY W. BROSIUS[3], JOSEPH M. DAVILA[2], ROGER J. THOMAS[2], VICENZO ANDREATTA[2] and HIROHISA HARA[4]

[1]*University of Alabama/MSFC, Huntsville, AL 35812, U.S.A.*
[2]*NASA/GSFC, Greenbelt, MD 20771, U.S.A.*
[3]*Ratheon STX, 4400 Forbes Blvd, Lanham, MD 20706, U.S.A.*
[4]*National Astronomical Observatory, Mitaka, Tokyo 181, Japan*

(Received 12 September 1997; accepted 15 December 1997)

Abstract. We investigate the possibility that strong EUV lines observed with the Goddard Solar EUV Rocket Telescope and Spectrograph (SERTS) provide good proxies for estimating the total coronal flux over shorter wavelength ranges. We use coordinated SERTS and *Yohkoh* observations to obtain both polynomial and power-law fits relating the broad-band soft X-ray fluxes to the intensities of Fe XVI 335 Å and 361 Å, Fe XV 284 Å and 417 Å, and Mg IX 368 Å measured with SERTS. We found that the power-law fits best cover the full range of solar conditions from quiet Sun through active region, though not surprisingly the 'cooler' Mg IX 368 Å line proves to be a poor proxy. The quadratic polynomial fits yield fair agreement over a large range for all but the Mg IX line. However, the linear fits fail conspicuously when extrapolated into the quiet-Sun regime. The implications of this work for the He II 304 Å line formation problem are also briefly considered.

1. Introduction

Spectra from the 1989 flight of the Goddard Solar EUV Rocket Telescope and Spectrograph (SERTS) yield intensity ratios between the most active and the quietest solar regions of 48 in the 335 Å line and 47 in the 361 Å line of Fe XVI, respectively (Jordan *et al.*, 1993). These values are comparable to the factor of 50 for the total coronal flux ratio between active-region and quiet-Sun conditions, estimated by Withbroe and Noyes (1976) from *Skylab* observations. The *Skylab* ratio was based on observations made by the X-ray Spectrographic Telescope, an instrument that provided several filters capable of observing soft X-ray radiation over the wavelength range of 3–60 Å (Vaiana *et al.*, 1973). This similarity suggests a quantitative relationship that could permit the use of individual EUV line intensity measurements as proxies for total coronal flux over important broad wavelength intervals. We report here on a test of this hypothesis, comparing EUV line intensities obtained during the 1993 flight of SERTS with simultaneous observations of the soft X-ray bands observed with the Soft X-ray Telescope (SXT) on *Yohkoh*. We also describe a preliminary comparison of nonsimultaneous SERTS and SOHO/CDS observations relevant to assessing the He II photoionizing radiation.

Solar Physics **180:** 179–191, 1998.

2. Instrument Descriptions and Observations

The SERTS instrument used to obtain these data and the manner in which they were obtained during the 1993 flight are described in detail in Brosius, Davila, and Thomas (1996). The observations were taken with a multilayer-coated grating flown for the first time in 1991 (Davila *et al.*, 1993) and optimized for the wavelengths around 300 Å (Thomas *et al.*, 1991). The entrance aperture of the quasi-stigmatic spectrograph allows only a selected portion of the solar image to pass through to the toroidal grating, which reimages it in each dispersed wavelength onto Kodak 101-07 EUV sensitive film. This entrance aperture was designed with a 'dumbbell' shape that permits spectra and spectroheliograms to be obtained simultaneously. Spectra are obtained along a narrow 4.9 arc min slit, which lies between the two wide lobes of areas 4.8×8.2 arc min and 4.8×7.6 arc min, respectively. Midway through the rocket flight the instrument pointing is changed by movement parallel to the narrow slit, so that spectra can be obtained from within two of the four regions covered by the wide lobes in the two pointing positions. These wide-lobe images are used for this collaborative study with *Yohkoh*.

The SERTS spatial resolution is about 5 arc sec, and the spectral resolution is about 55 mÅ, changing slightly in a known way along the narrow slit. The wavelength range covered is 235–450 Å. Brosius, Davila, and Thomas (1996) demonstrated that the relative line intensities are accurate to within 20% over 280 –420 Å. All of the SERTS lines we use for this study lie within that range. Thomas and Neupert (1994) estimate that the absolute radiometric accuracy over this range is better than a factor of 2. The wide-lobe SERTS images used for pixel-to-pixel comparison with *Yohkoh* images include some contribution from other weaker lines than those chosen for this study, but in all cases the contributions from these other lines are negligible except for the quietest regions studied.

The *Yohkoh*/SXT is most sensitive to coronal X-ray emission between 1.0 Å and 30 Å, though there is some rapidly declining sensitivity up to about 100 Å (Tsuneta *et al.*, 1991, Figure 8). The SXT is equipped with five different filters, each with a different plasma temperature-response function. Images were taken during the SERTS flight using both a thin-aluminum filter and an Al/Mg/Mn (sandwich) filter, which have the broadest temperature-response functions of the five. These two filters provide a broad-band response to emission from solar plasma with temperatures greater than about 1×10^6 K. Although it is most sensitive to plasma at temperatures of $3–5 \times 10^6$, the SXT also yields information on quiet-Sun soft X-ray emission.

For the study of coronal flux proxies, we used SERTS wide-field images in the lines of Fe XVI at 335 and 361 Å, of Fe XV at 284 and 417 Å and of Mg X at 368 Å. We also obtained wide-field images in the He II resonance line at 304 Å for other reasons discussed below. These observations were made in the second pointing position during the flight. Following microdensitometry of the film and intensity calibration, these images were coregistered with *Yohkoh*/SXT images of

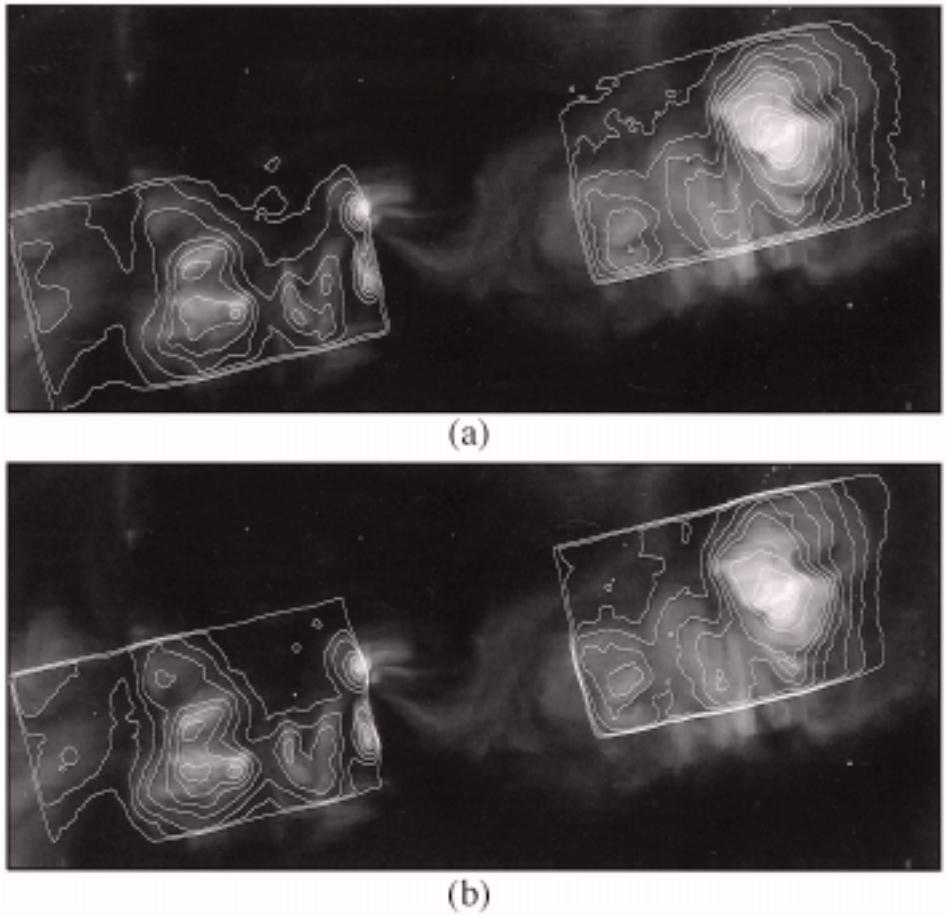

Figure 1. The SERTS 'dumbell' slit projected onto the *Yohkoh* image for the 1993 observations reported in this paper. (a) shows contours in the measured SERTS Fe XVI 335 Å intensity and (b) shows contours in the corresponding 284 Å intensity. The two instruments' resolutions are different, which leads to the difference in the sharpness of the features.

the same solar region. The coaligned *Yohkoh* images were masked and rebinned to match exactly the SERTS field-of-view and pixel size. It was then straightforward to compare pixel-to-pixel the calibrated SERTS intensities with the corresponding *Yohkoh* flux values. The SXT observations used for the analysis reported here were taken with the thin-aluminum filter, because of that filter's superior sensitivity. Observations taken with the sandwich filter, when tested, yielded similar results.

Examples of our coaligned data are shown in Figure 1, where contours of SERTS Fe XV 284 Å and Fe XVI 335 Å are projected onto the corresponding *Yohkoh*/SXT observations.

Table I
Average integrated intensities (ergs cm^{-2} s^{-1} st^{-1}) for active region and quiet-Sun areas observed with SERTS-93, from Brosius, Davila, and Thomas (1996)

Spectral line	Ave active region	Ave quiet-Sun	Ratio of Ave AR/QS
Fe XVI 335 Å	$4.09 \pm 0.47 \times 10^3$	$1.63 \pm 0.19 \times 10^2$	25.09
Fe XVI 361 Å	$2.04 \pm 0.23 \times 10^3$	$7.72 \pm 0.89 \times 10^1$	26.24
Fe XV 284 Å	$5.78 \pm 0.65 \times 10^3$	$5.00 \pm 0.57 \times 10^2$	11.56
Fe XV 417 Å	$2.41 \pm 0.30 \times 10^2$	$1.30 \pm 0.20 \times 10^1$	18.56
Mg X 368 Å	$9.43 \pm 1.01 \times 10^2$	$1.82 \pm 0.21 \times 10^2$	5.18
He II 304 Å	$3.34 \pm 0.38 \times 10^4$	$6.94 \pm 0.78 \times 10^3$	4.81

3. The Comparison of SERTS and *Yohkoh*/SXT Observations

The main results of the image coregistration and intensity/flux comparisons are exhibited as scatter plots in Figures 2–5. We include the results of both power-law and polynomial fitting routines in Figure 2, and give only the results of the more satisfactory power-law fitting in Figures 3–5. Results illustrated are for the lines of Fe XVI 335 Å and 361 Å, Fe XV 284 Å, and also, for reasons given in Section 4, He II 304 Å. Fits were also obtained for Fe XV 417 Å and for Mg IX 368 Å, but these results proved less satisfactory and are not illustrated.

The average quiet-Sun and active-region intensities from Brosius, Davila, and Thomas (1996) are identified in Figures 2–5, to give some idea of the range over which the fitting was done. These values, plus those for the other lines fitted, are reproduced in Table I. Figure 2 shows that the Fe XVI 335 Å line is a reasonably good proxy over most of the range fitted, but that a linear fit can err by as much as an order of magnitude if the Sun is very quiet. The same result is obtained for the other highly ionized iron lines of Figures 3 and 4. We note that the increase in intensity of the Fe XVI lines from active region to quiet-Sun is only slightly greater than half the values obtained from the SERTS-89 flight. This is almost certainly due to the fact that all the strong coronal line intensities observed in NOAA active region 7563 during the 1993 flight were weaker than the corresponding lines observed in NOAA 5464 during 1989; i.e., NOAA 7563 was a 'weaker' active region overall. The coefficients of the different power-law fits for all the lines treated appear in Table II, and those for the polynomial fits are shown in Table III. First-order power-laws were fit to the data with SERTS intensities greater than a critical intensity at which the scatter between the *Yohkoh* and SERTS intensities was small. The quadratic fits used all the data.

The slopes of the first-order power-law fits in Table III yield useful information on how the different SERTS lines, formed at different temperatures, compare to the *Yohkoh*/SXT intensities. The greater the difference of the different lines' temperature-response functions from the *Yohkoh* functions (which peak at 3×10^6 K), the greater the slope. This makes sense, since we expect the ratio of intensities

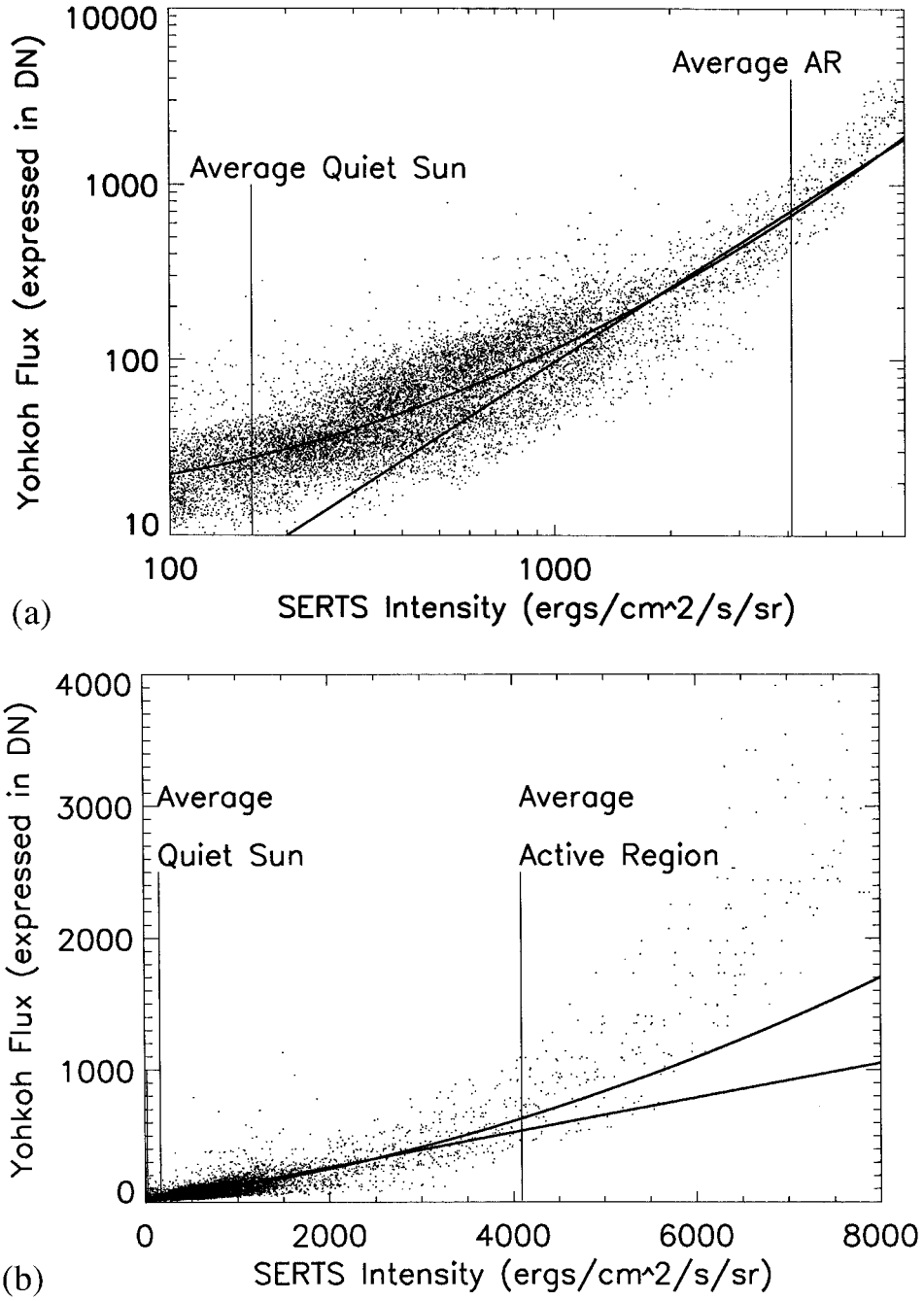

Figure 2. Scatter plots of SERTS Fe XVI 335 Å intensity versus *Yohkoh*/SXT flux with both power-law fits (a), and polynomial fits (b). The fits were derived by a least-square method over the intensity ranges as discussed in the text. The coefficients of the fits are given in Tables II and III. The fits for (a) for the brighter pixels are to within a factor of 50% of the observed spread of the data while for the dimmer pixels the fit is within a factor of 3. The lack of one-to-one correspondence in the intensity can be attributed to a combination of instrument uncertainties and the lack of a one-to-one correspondence of intensity to temperature.

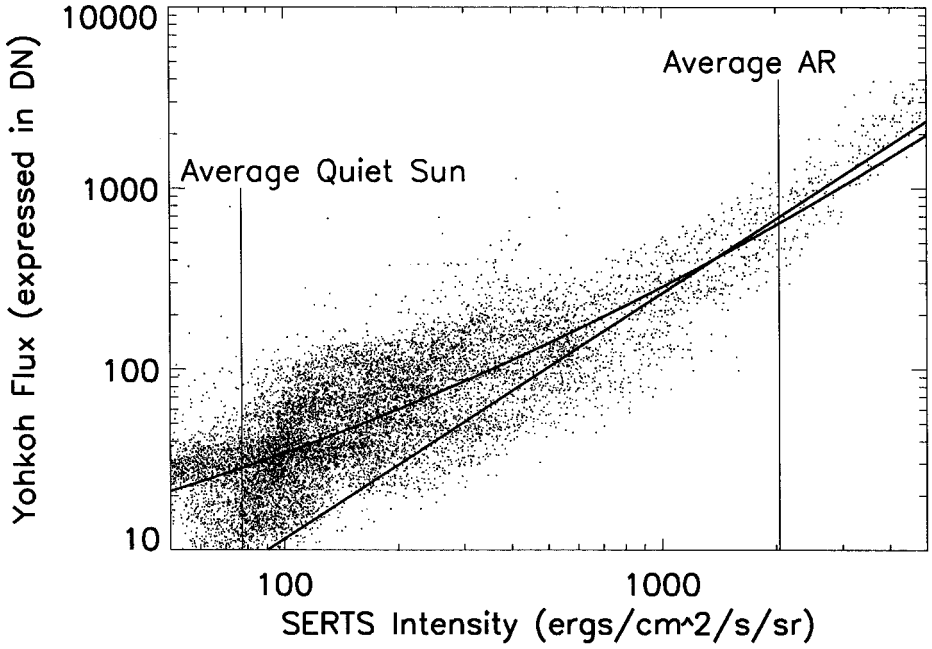

Figure 3. This figure is the same as Figure 2(a) except the Fe XVI 361 Å spectral line is fitted.

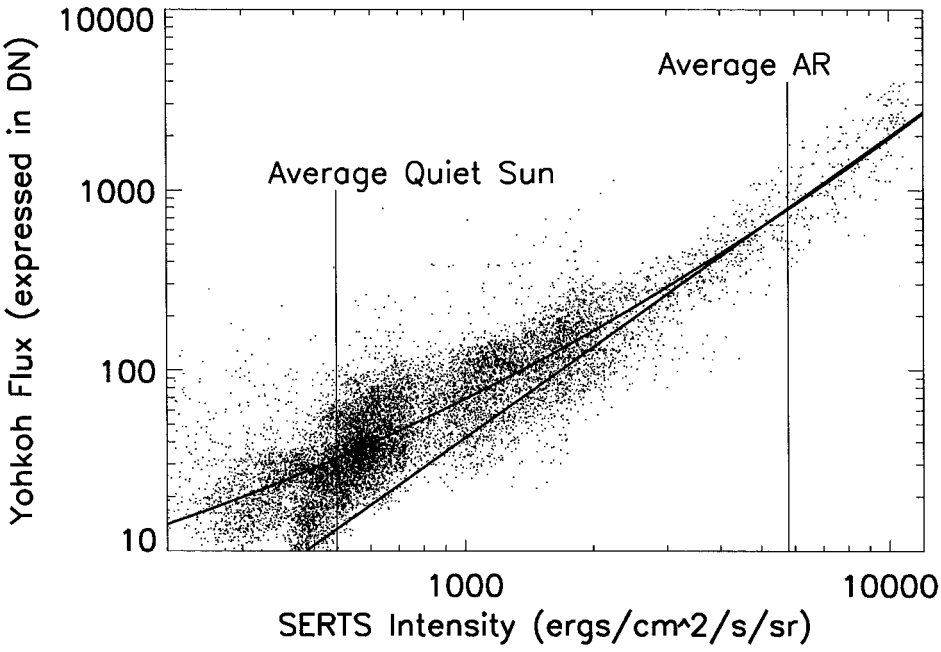

Figure 4. This figure is the same as Figure 2(a) except the Fe XV 284 Å spectral line is fitted.

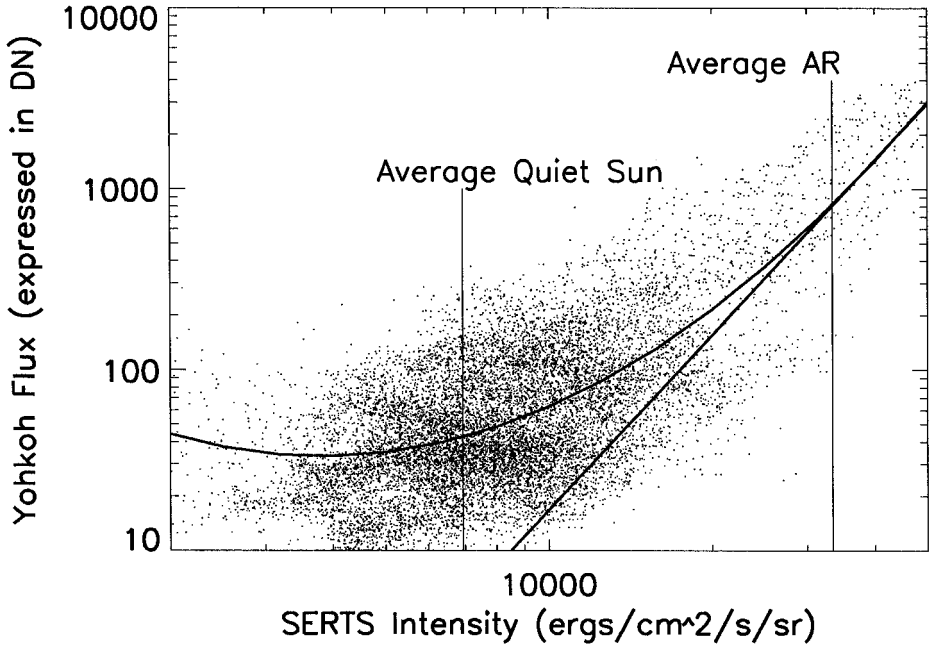

Figure 5. This figure is the same as Figure 2(a) except the He II 304 Å spectral line is fitted.

Table II
Coefficients for the polynomial fits

Spectral line	$A+Bx$		$A+Bx+Cx^2$			App. formation temperature
	A	B	A	B	C	
Fe XVI 335 Å	0.64	0.13	19	0.086	1.6	2.5×10^6
Fe XVI 361 Å	12	0.28	23	0.21	5.0×10^{-5}	2.5×10^6
Fe XV 284 Å	28	0.11	12	0.050	1.4×10^{-5}	2.0×10^6
Fe XV 417 Å	−26	3.6	18	1.4	-1.4×10^{-2}	2.0×10^6
Mg X 368 Å	−290	1.4	250	−1.6	3.7×10^{-3}	1.0×10^6
He II 304 Å	−130	0.02	129	−0.019	1.3×10^{-6}	8.0×10^4

Note: The standard deviation of the *Yohkoh* intensity for a given SERTS intensity is roughly a factor of 1.6 for average quiet-Sun conditions and 1.4 for average active region intensities.

from the higher temperature lines to the lower temperature lines to increase as the temperature increases. As expected, the higher temperature lines are better proxies for coronal radiation, at least in the *Yohkoh* energy range.

Figure 6 shows that bright regions are normally hot with a narrow range of temperatures (2.5×10^6–3×10^6 K) while dim regions have a wider range of temperatures (1.5×10^6–3×10^6 K). Thus, while there is no one-to-one correspondence of temperature to brightness, the average temperature increases as the brightness increases and the range of temperatures for a given brightness level decreases. The

Table III
Coefficients for the power-law fits

Spectral line	$A + B\log(x)$		$A + B\log(x) + C\log(x)^2$			App. formation temperature
	A	B	A	B	C	
Fe XVI 335 Å	−2.3		1.13	−0.41	0.086	2.5×10^6
Fe XVI 361 Å	−1.7	1.36	0.90	−0.14	0.038	2.5×10^6
Fe XV 284 Å	−3.4	1.67	0.24	0.06	0.021	2.0×10^6
Fe XV 417 Å	−0.91	1.65	1.65	−0.49	0.138	2.0×10^6
Mg X 368 Å	−3.9	2.30	3.27	−2.27	0.506	1.0×10^6
He II 304 Å	−12	3.22	4.27	−2.11	0.289	8.0×10^4

Note: The standard deviation of the *Yohkoh* intensity for a given SERTS intensity is roughly a factor of 1.6 for average quiet-Sun conditions and 1.4 for average active region intensities.

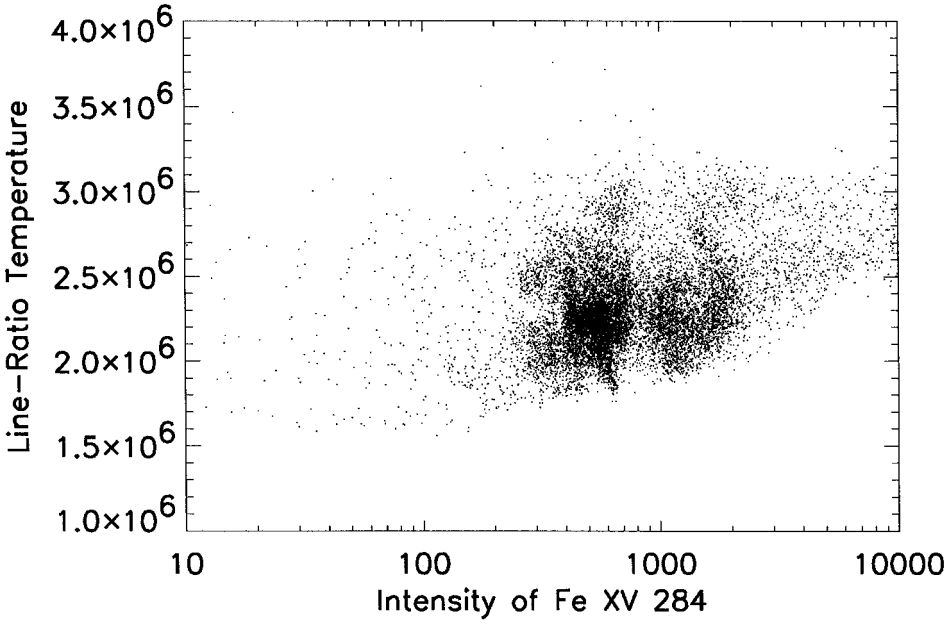

Figure 6. Scatter plot of line-ratio temperature of Fe XVI 361 Å to Fe XV 284 Å. The observed temperature spread is clearly wider for dim pixels than for bright ones, with few pixels having line-ratio temperatures of much above 3×10^6 K.

temperature dependence as a function of brightness in Figure 6 shows that these highly ionized iron lines are better proxies for active regions than for quiet Sun conditions. Both of these lines yield reasonable estimates of SXT fluxes (again see Figures 3 and 4), but the range of temperatures and estimated fluxes decreases as the region observed becomes more active.

The intensity of a SERTS spectral line or an SXT bandpass can be written as

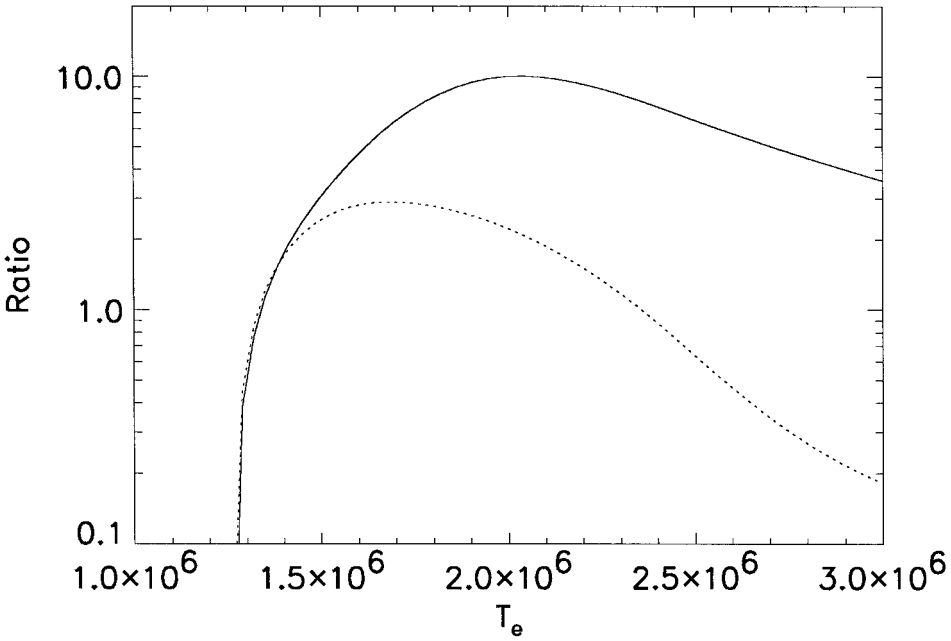

Figure 7. The theoretical intensity ratio of Fe XV 284 Å, and Fe XVI 361 Å vs *Yohkoh* SXT flux observed with the thin aluminum filter as a function of temperature. Both ratios are double value with the Fe XV (dotted) peaking at 1.5×10^6 and the Fe XVI (solid) peaking at 2×10^6 K. Below 1.4×10^6 K both ratios changes rapidly. Due to absolute calibration concerns between the two instruments these theoretical intensity ratios cannot be used to measure the temperatures.

$$I(T, \eta) = G(T)\eta \,, \tag{1}$$

where I is the intensity, G is the plasma emissivity in either a single SERTS line or over a SXT wavelength band, and η is the emission measure. Line-ratio diagnostics assumes that all of the emission from the two different spectral regimes is emitted from the same volume of isothermal plasma, so both have the same emission measure η. This is a reasonable approximation for these iron lines and SXT bandpasses. The intensity ratio of the two different spectral regimes then becomes

$$R_{1,2} = \frac{I_1}{I_2} = \frac{G_1(T)}{G_2(T)} \,. \tag{2}$$

We can obtain the quantities $G_1(T)$ and $G_2(T)$ from Brickhouse, Raymond, and Smith (1995) and Tsuneta *et al.* (1991). Figure 7 plots $R_{1,2}$ as a function of temperature for the lines Fe XV 284 Å and Fe XVI 361 Å vs the wavelength band observed by *Yohkoh* with the thin aluminum filter.

The SERTS spectral intensity would be a perfect proxy for the SXT flux if either of two conditions were met. Either the relation between intensity and temperature

is single valued, or $G_1(T)$ and $G_2(T)$ have the same temperature dependence. Clearly neither condition is met. However, Figure 6 has already shown that the spread of SXT fluxes for given intensities of Fe XV 284 Å and Fe XVI 361 Å is comparatively narrow, approximately a factor of 2. This is not surprising because the plasma emissivities peak in all three cases over a similar high temperature range. Figure 7 shows that there is also a greater change in the ratio $R_{1,2}(T)$ over quiet-Sun conditions than for a broad range of active regions conditions. One would also expect the concave shape exhibited by the linear power-law fits illustrated in Figures 2–4, from the theoretical intensity ratios of Figure 7, where the ratio is smaller for the higher and lower temperatures than for the intermediate temperatures.

4. Discussion, Including the Helium 304 Å Problem

The primary objective of this study is to assess the value of several strong spectral lines observed with the SERTS as 'proxies' for solar coronal flux over some definable range of solar conditions.

We demonstrate here that the second-order power-law fits for the highly ionized iron lines illustrated provide reasonably good proxies over a broad range of coronal intensities, and predict the *Yohkoh* broad-band soft X-ray fluxes to within 50% for active regions or a factor of 3 for quiet-Sun conditions. All other fits were less satisfactory, for various reasons. In particular, use of a linear approximation with the Fe XVI lines underestimates the quiet-Sun soft X-ray intensity by as much as an order of magnitude.

Two equal volumes of coronal plasma at the same temperature might still yield a different ratio of 'proxy' intensity to coronal flux if there are different densities in the two volumes, or if there are different elemental abundances. Using a spectral line whose emissivity is comparatively density insensitive, such as Fe XVI 361 Å or Fe XV 284 Å, addresses the first concern.

The second concern is probably more serious, as coronal abundances are known to vary from one structure to another (Meyer, 1985). This effect can be minimized if we use only spectral lines from an element that dominates the plasma emission over the bandpass of interest. According to Cook *et al.* (1989), iron dominates the emission of solar plasma for temperatures greater than 300 000 K. Adding in only the other elements with a low first ionization potential (FIP) less than 10 eV, this domination continues up to temperatures of several million degrees until bremsstrahlung radiation becomes significant, even for photospheric abundances. Cook *et al.* also show that a variation of a factor of four in the low-FIP elemental abundance would produce only a variation of 50% in the ratio of iron-line emission to total emission. In contrast, a variation of a factor of four in the abundance of high-FIP elements (FIP $>$ 10 eV) could introduce nearly a factor of four variation in this latter ratio. However, one should note that spectra from very low-FIP elements

(FIP $<$ 6.1 eV) such as Al, Ca, and Na would be a poor choice for assessing the coronal flux, as previous work has shown that they can be enhanced in the corona compared to the other low-FIP elements by as much as a factor of four (Falconer, Davila, and Thomas, 1997).

In addition to fitting the SERTS coronal line intensities against *Yohkoh*/SXT fluxes, we also fitted the SERTS He II 304 Å line, in an effort to determine if any quantitative relationship existed between these relatively 'hot' coronal radiations and the transition region 304 Å line, whose mechanism of formation remains a subject of current research. This fit exhibits a larger departure from linearity than any of the highly ionized iron cases, as illustrated in Figure 5. However, the soft X-ray fluxes measured by *Yohkoh* lie far from the He II ionization edge of 228 Å. It would be far more meaningful to correlate simultaneous cospatial 304 Å intensities with intensities in the strong iron lines that lie just below this ionization edge, to gain insight into the role of photoioization-recombination ($p - r$) in the formation of the 304 Å line.

Figure 8 provides us with a rough estimate of what these ionizing fluxes are. Both the quiet-Sun and active-region spectra shown in Figure 8 were obtained on 2 September 1996, with the Coronal Diagnostic Spectrometer (CDS) Grazing-Incidence Spectrometer (GIS) on the Solar and Heliospheric Observatory (SOHO). One sees an increase of over an order of magnitude in the number of counts recorded for the active-region spectrum over the quiet-Sun spectrum, in the strong ionized-iron lines lying just short of 228 Å.

One would expect such an increase in the most effective photoionizing radiation to yield a larger than observed increase in the quiet Sun to active-region 304 Å intensity in SERTS 304 data of Figure 5, unless there are large effects due to absorption of 304 Å photons within the atmosphere. One possibility is that the $p - r$ mechanism dominates the line formation everywhere, and that there are indeed large saturation effects in the active region, but this contradicts results supporting collisional excitation in at least the quiet Sun (Jordan *et al.*, 1993). These considerations, taken together, suggest that collisional excitation of the 304 Å line may dominate over $p - r$ in active regions as well as in the quiet Sun, especially in view of the large increase in electron density found in active regions, which causes a corresponding (linear) increase in the collision-dominated source term in the line source function. We are hopeful that research currently underway using SERTS, SOHO, and ground-based observations will further clarify this picture.

It is somewhat speculative at this stage whether Extreme Ultraviolet Explorer (EUVE) observations of the lines Fe XV 284 Å and Fe XVI 335 Å and 361 Å might be useful for estimating total coronal fluxes for a number of other late-type stars, but the data are available. Since the resolution of the spectrometer over the wavelength range 70–760 Å is about 200 (Bowyer and Molina, 1991), blending will introduce some error, but not necessarily a serious one for total flux estimations. A number of 'cool' stars for which these lines have been observed are reviewed in Jordan (1996). These include Procyon, Chi Boo A (+B), and Capella. While current work

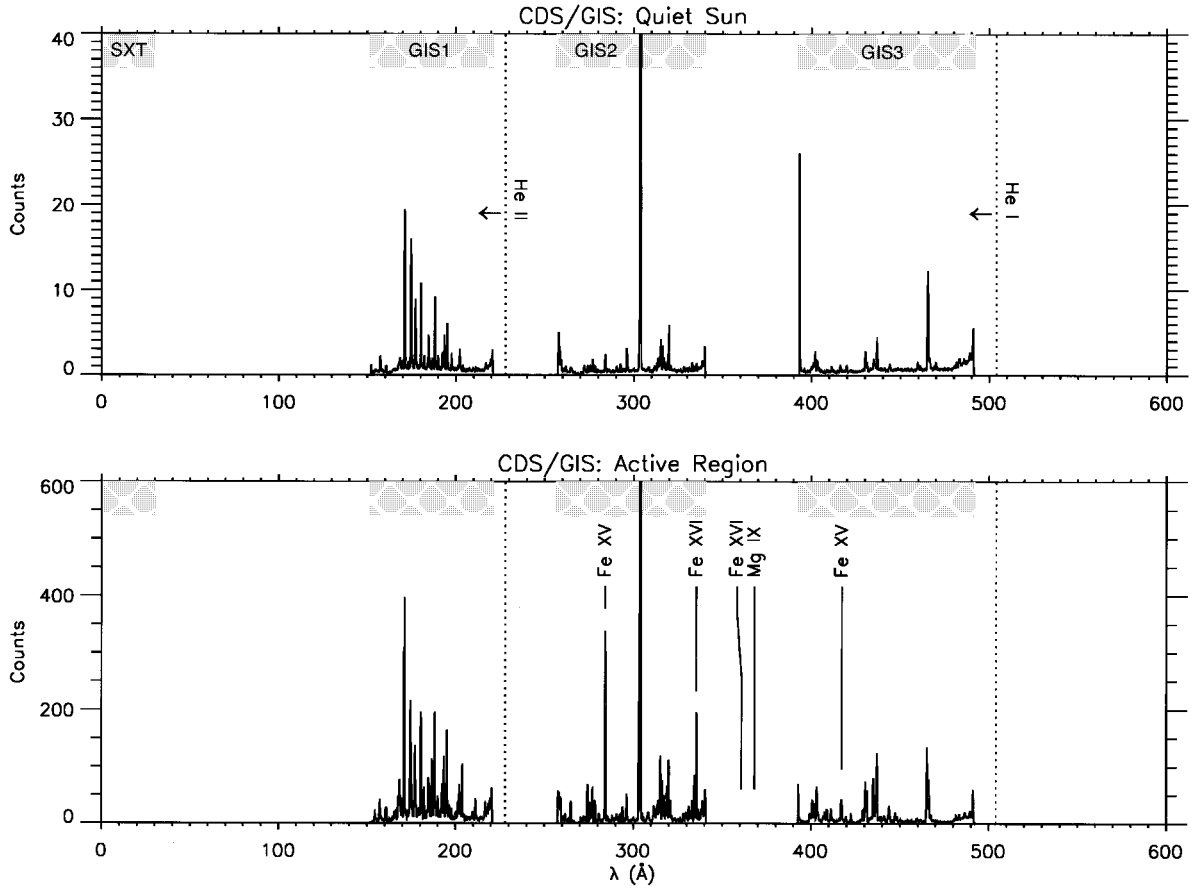

Figure 8. Preliminary CDS GIS averaged spectra from both quiet-Sun and active region. The GIS Band 1 spectrum is most relevant to He II ionization, which occurs at wavelengths short of 228 Å. The quiet spectrum was averaged over a fairly uniform area of $30'' \times 30''$ near disk center. The active region observed was NOAA 7986. In the active region scan, we have included only those pixels whose Fe IX 171 Å intensity exceeded 80% of the peak intensity in the same line. The SERTS lines discussed in this paper are located on the figure at the appropriate wavelengths.

features fairly straightforward spectroscopic diagnostics, future efforts to assess line-formation mechanisms might find the use of these lines as proxies for total coronal flux useful.

Acknowledgements

The SERTS program is supported by NASA grant 682–344–17–38. We gratefully acknowledge the use of the *Yohkoh*/SXT observations. The authors thank CDS Co-Investigator Andrzej Fludra for his assistance. JWB acknowledges NASA support through contracts NASW-5020 and NASW-96006. This work was performed while D. A. Falconer held a National Research Council-MSFC Research Associateship and V. Andretta held a National Research Council-GSFC Research Associateship. We thank the referee for several useful suggestions to clarify the significance of the results.

References

Bowyer, S. and Molina, R. F.: 1991, in R. F. Molina and S. Bowyer (eds.), *Extreme Ultraviolet Astronomy*, Pergamon Press, New York, p. 397.

Brickhouse, N. S., Raymond, J. C., and Smith, B. W.: 1995, *Astrophys. J. Suppl. Series* **97**, 551.

Brosius, J. W., Davila, J. M., and Thomas, R. J.: 1996, *Astrophys. J. Suppl. Series* **106**, 143.

Cook, J. W., Cheng, C.-C., Jacobs, V. L., and Antiochus, S. K.: 1989, *Astrophys. J.* **338**, 1176.

Davila, J. M., Thomas, R. J., Thompson, W. T., Keski-Kuha, R. A. M., and Neupert, W. M.: 1993, in E. Silver and S. Kahn (eds.), *UV and X-Ray Spectroscopy of Laboratory and Astrophysical Plasma*, Cambridge University Press, Cambridge, p. 301.

Falconer, D. A., Davila, J. M., and Thomas, R. J.: 1997, *Astrophys. J.* **482**, 1050.

Jordan, C.: 1996, in S. Bowyer and R. F. Molina (eds.), *Astrophysics in the Extreme Ultraviolet*, Kluwer Academic Publishers, Dordrecht, Holland, p. 81.

Jordan, S. D., Thompson, W. T., Thomas, R. J., and Neupert, W. M.: 1993, *Astrophys. J.* **406**, 346.

Thomas, R. J. and Neupert, W. M.: 1994, *Astrophys. J. Suppl.* **91**, 461.

Thomas, R. J., Keski-Kuha, R. A. M., Neupert, W. M., Condor, C. E., and Gum, J. S.: 1991, *Appl. Optics* **30**, 2245.

Tsuneta, S., Acton, L., Bruner, M., Lemen, J., Brown, W., Caravalho, R., Catura, R., Freedland, S., Jurcevich, B., Morrison, M., Ogawara, Y., Hirayama, T., and Owens, J.: 1991, in Z. Švestka and Y Uchida (eds.), 'The Soft X-Ray Telescope for the Solar-A Mission', *The Yohkoh (Solar-A) Mission*, Kluwer Academic Publishers, Dordrecht, Holland, p. 37.

Vaiana, G. S., Davis, J. M., Giacconi, R., Krieger, A. S., Silk, J. K., Timothy, F., and Zombeck, M.: 1973, *Astrophys. J.* **185**, L47.

Withbroe, G. L. and Noyes, R. W.: 1977, in G. Burbidge (ed.), *Ann. Rev. Astron. Astrophys.* **16**, 363.